

We are IntechOpen, the world's leading publisher of Open Access books Built by scientists, for scientists

6,900

Open access books available

186,000

International authors and editors

200M

Downloads

Our authors are among the

154

Countries delivered to

TOP 1%

most cited scientists

12.2%

Contributors from top 500 universities



WEB OF SCIENCE™

Selection of our books indexed in the Book Citation Index
in Web of Science™ Core Collection (BKCI)

Interested in publishing with us?
Contact book.department@intechopen.com

Numbers displayed above are based on latest data collected.
For more information visit www.intechopen.com



Vector Correlations in Collision of Atom and Diatomic Molecule

Xian-Fang Yue
Jining University
China

1. Introduction

The use of crossed molecule beam (CMB) and polarized laser techniques has allowed the precisely measurements of the vector correlations in atom and diatomic molecule collision reactions. There are a variety of experimental studies aiming at exploring the vector correlations underlying a collision reaction.[1-15] To name a few are those of Zare and co-workers, [1-3] those of Herschbach and co-workers [4-5], those of Fano and co-workers [6], as well as those of Han and co-workers [7-9]. These experimental investigations impelled the development of theoretical methods to simulate the measured profiles and to explore the unmeasured ones. Generally, theoretical explorations on vector correlations of collision reactions fall into two categories: one is the reagent k - j , j - k - k' vector correlations, and the other is the product k - j' , k - k' - j' vector correlations. Where k/k' and j/j' denotes the relative velocity of reagent/product and reagent/product rotational angular momentum in the centre of mass (CM) frame. As reported in many previous papers, both of the quantum scattering and the quasi-classical trajectory (QCT) calculations can be used to investigate the vector correlations. In this chapter, we report the product k - j' , k - k' - j' vector correlations of the $N(^2D) + H_2(v, j) \rightarrow NH(v', j') + H$ collision reactions with the QCT method.

The $N(^2D) + H_2 \rightarrow NH + H$ collision reaction plays an important role in the chemistry of nitrogen containing fuels and of nitrogen in the atmosphere [16]. It has attracted many investigations from not only experimental viewpoints [17-25], but also theoretical viewpoints [26-37]. Experimentally, Suzuki et al. [17] measured the rate constants for this reaction by employing a pulse radiolysis-resonance absorption technique at temperatures between 213 and 300 K. They found that the temperature dependence of the rate constants exhibits an Arrhenius behavior. Umemoto and coworkers [18-20] measured the vibrational and rotational state distributions of the nascent NH and ND molecules formed in the $N(^2D) + H_2$ and $N(^2D) + D_2$ reactions. In their experiments, the $N(^2D)$ atoms were generated by two-photon dissociation of NO, while the nascent NH and ND molecules were detected by laser-induced fluorescence (LIF) technique. They found that the nascent vibrational distributions have $NH(v''=1)/NH(v''=0) = 0.8 \pm 0.1$ and $ND(v''=1)/ND(v''=0) = 1.0 \pm 0.1$, and that the rotational populations of these vibrational states are broad and hot. More recently, Casavecchia et al. [21-25] carried out a series of experimental and theoretical studies on the $N(^2D) + H_2$ and $N(^2D) + D_2$ reactions. They have measured the angular and velocity distributions of the nascent NH and ND products in the title reactions under CMB experiments with mass spectrometric detection technique.

Theoretically, Honvault and Launay [26] carried out the first accurate quantum mechanics (QM) calculations of the $N(^2D) + H_2$ reaction on the Pederson et al. PES [27] with the hyperspherical method. They calculated the vibrationally and rotationally state resolved integral cross sections at collision energies of 1.6, 2.5, and 3.8 kcal/mol. A forward-backward symmetry was also found in their differential cross sections (DCS) calculations, which indicates that a complex of NH_2 is formed in the reaction. In a recent work, Ho et al. [28] improved and refined the Pederson et al. PES [27], and developed a more accurate adiabatic ground $1^2A''$ PES. The new PES is fitted by a set of 2715 ab initio points resulting from the multireference configuration interaction (MRCI) calculations and a better algorithm. Moreover, the new PES is free of spurious small scale features and is in much better agreement with the ab initio calculations, especially in key stationary point regions including the C_{2v} minimum, the C_{2v} transition state, and the N-H-H linear barrier. Employing this new PES, both QM [29-32] and QCT [28, 31-33] calculations have been performed for the title reactions.

Most of previous studies focused on the calculations of the reaction probabilities, integral cross sections and thermal rate constants. Very few investigations paid attention to the vector properties calculations for the $N(^2D) + H_2$ reactions. In this chapter, we present a much detailed calculations on the vector correlations of this collision reaction.

2. Methodology and theory

2.1 Quasi-classical trajectory calculations

The QCT calculation method is the same as that in Refs. [38-42]. Six-order symplectic integration was used in the QCT calculations, in which the classical Hamilton's equations are integrated numerically for motion in three dimensions. In a given Hamiltonian system whose Hamiltonian can be partitioned, i.e., written as $H = T(p) + U(q)$, we define the derivative terms in the Hamiltonian movement equations as $hq_i = \partial H / \partial p_i$ for the generalized momentum, and $hp_i = \partial H / \partial q_i$ for the generalized coordinates; let dt be the full time step. The algorithm can be expressed as [42]

do $i = 0, 1, 2, \dots, n - 2, n - 1$

$$p = p + dt a(2i) hp$$

$$q = q + dt a(2i + 1) hq$$

enddo

$$p = p + dt a(2n) hp. \tag{1}$$

The last step can be concatenated with the first step in a continuing calculation. Then there are $2n$ substeps in every step, where n is 8 for six-order symplectic integrator. Thus, the number of the calling to the potential derivatives is also n . The coefficients are defined by $2n + 1$ values of $a(i)$, which is taken directly from Ref. [43-44] without revision.

The accurate $1^2A''$ state PES constructed recently by Ho et al. [28] is employed for the $N(^2D) + H_2 \rightarrow NH + H$ calculations. The full potential is written in terms of a many body expansion:

$$V(R_{\text{NH}_a}, R_{\text{NH}_b}, R_{\text{HH}}) = V^{(1)} + V_{\text{NH}}^{(2)}(R_{\text{NH}_a}) + V_{\text{NH}}^{(2)}(R_{\text{NH}_b}) + V_{\text{HH}}^{(2)}(R_{\text{HH}}) + V^{(3)}(R_{\text{NH}_a}, R_{\text{NH}_b}, R_{\text{HH}}), \quad (2)$$

Where the one-body term $V^{(1)}$ defines the zero of energy as the three-atom limit and the two-body terms $V_{\text{NH}}^{(2)}$ and $V_{\text{HH}}^{(2)}$ represent the energy of H + NH and N + H₂, respectively. The two-body functions are interpolated from separate calculations of the two-body potentials using the reciprocal power radial kernel. The three-body function $V^{(3)}(R_{\text{NH}_a}, R_{\text{NH}_b}, R_{\text{HH}})$ in the coordinate system is interpolated from the differences between the ab initio data and the corresponding one- and two-body sums. During reactive encounter, the total angular momentum is conserved

$$L + j = L' + j', \quad (3)$$

where L and L' are the reagent and product orbital momenta, respectively. In the mass weighted coordinates, the rotational angular momentum (AM) of reagent molecule H₂ is

$$j = \mu_{\text{HH}} \mathbf{R}_{\text{HH}} \times \dot{\mathbf{R}}_{\text{HH}} = \sqrt{j(j+1)}\hbar, \quad (4)$$

and reagent orbital AM is

$$l = \mu_r \mathbf{R}_{\text{N-HH}} \times \dot{\mathbf{R}}_{\text{N-HH}} = \sqrt{l(l+1)}\hbar. \quad (5)$$

Accordingly, the product rotational AM is

$$j' = \mu_{\text{NH}} \mathbf{R}_{\text{NH}} \times \dot{\mathbf{R}}_{\text{NH}} = \sqrt{j'(j'+1)}\hbar, \quad (6)$$

and the product orbital AM is

$$l' = \mu_p \mathbf{R}_{\text{NH-H}} \times \dot{\mathbf{R}}_{\text{NH-H}} = \sqrt{l'(l'+1)}\hbar. \quad (7)$$

Where μ_r and μ_p are reagent and product reduced masses, respectively. The Hamilton's motion equation is solved by the symplectic integration method. The accuracy of the numerical integration is verified by checking the conservations of the total energy and the total angular momentum for every trajectory. In the calculation, batches of 1×10^5 trajectories are run for each reaction and the integration step size is chosen to be 0.1 femtosecond (fs). The trajectories start at an initial distance of 15 Å between the N atom and the center of the mass of the H₂ molecules. The impact parameter b is optimized through the repeated computation with 1×10^5 trajectories for all of the present studies. The maximum impact parameter b_{max} was obtained when there is no reactive trajectory any more, if a tiny larger value of b is done. All the optimized maximum impact parameters used for the present study are displayed in Table 1.

2.2 Polarization-dependent differential cross-sections (PDDCSs)

The CM frame was used as the reference frame in the present work, which is depicted in Figure 1. The reagent relative velocity vector k is parallel to the z-axis. The x-z plane is the

scattering plane which contains the initial and the final relative velocity vectors, k and k' . θ_t is the angle between the reagent relative velocity and product relative velocity (so-called scattering angle). θ_r and ϕ_r are the polar and azimuthal angles of the final rotational angular momentum j' .

The distribution function $P(\theta_r)$ describing the k - j' correlation can be expanded in a series of Legendre polynomials as [38-41]

$$P(\theta_r) = \frac{1}{2} \sum_k [k] a_0^k P_k(\cos \theta_r), \quad (8)$$

where $[k] = 2k + 1$. The a_0^k coefficients are given by

$$a_0^k = \langle P_k(\cos \theta_r) \rangle. \quad (9)$$

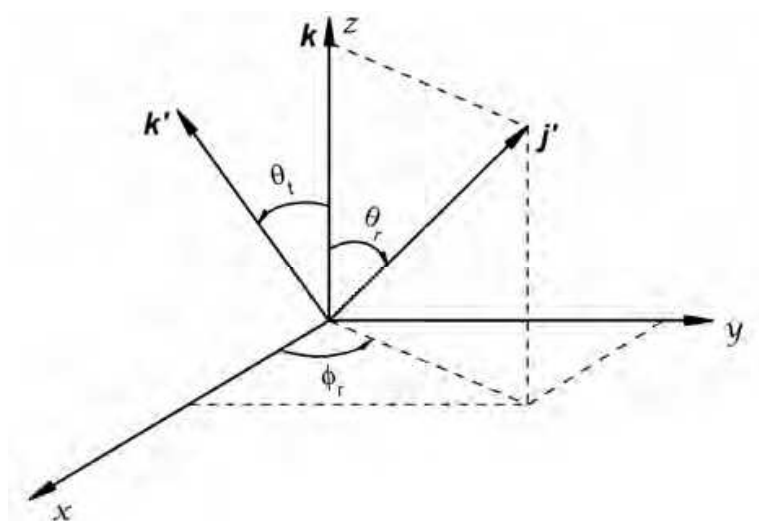


Fig. 1. Center-of-mass coordinate system used to describe the k , k' and j' correlations.

The expanding coefficients a_0^k are called orientation (k is odd) and alignment (k is even) parameters.

The dihedral angle distribution function $P(\phi_r)$ describing k - k' - j' correlation can be expanded in Fourier series as [38-41]

$$P(\phi_r) = \frac{1}{2\pi} \left(1 + \sum_{\text{even}, n \geq 2} a_n \cos n\phi_r + \sum_{\text{odd}, n \geq 1} b_n \sin n\phi_r \right), \quad (10)$$

where

$$a_n = 2 \langle \cos n\phi_r \rangle, \quad (11)$$

$$b_n = 2 \langle \sin n\phi_r \rangle. \quad (12)$$

In this calculation, $P(\phi_r)$ is expanded up to $n = 24$, which shows good convergence. The joint probability density function of angles θ_r and ϕ_r , which determine the direction of j' , can be written as

$$\begin{aligned}
 P(\theta_r, \phi_r) &= \frac{1}{4\pi} \sum_{kq} [k] a_q^k C_{kq}(\theta_r, \phi_r)^* \\
 &= \frac{1}{4\pi} \sum_k \sum_{q \geq 0} [a_{q\pm}^k \cos q\phi_r - a_{q\mp}^k i \sin q\phi_r] C_{kq}(\theta_r, 0).
 \end{aligned} \tag{13}$$

this calculation, the polarization parameter is evaluated as

$$a_{q\pm}^k = 2 \langle C_{k|q|}(\theta_r, 0) \cos q\phi_r \rangle, \text{ k is even,} \tag{14}$$

$$a_{q\pm}^k = 2i \langle C_{k|q|}(\theta_r, 0) \sin q\phi_r \rangle, \text{ k is odd.} \tag{15}$$

In the calculation, $P(\theta_r, \phi_r)$ is expanded up to $k = 7$, which is sufficient for good convergence.

The full three-dimensional angular distribution associated with $k-k'j'$ correlation can be represented by a set of generalized polarization-dependent differential cross-sections (PDDCSs) in the CM frame. The fully correlated CM angular distribution is written as [38-41]

$$P(\omega_t, \omega_r) = \sum_{kq} \frac{[k]}{kq} \frac{1}{4\pi} \frac{d\sigma_{kq}}{\sigma d\omega_t} C_{kq}(\theta_r, \phi_r)^*, \tag{16}$$

Where the angles $\omega_t = \theta_t, \phi_t$ and $\omega_r = \theta_r, \phi_r$. σ is the integral cross section. $C_{kq}(\theta_r, \phi_r)$ are

modified spherical harmonics. $\frac{1}{\sigma} \frac{d\sigma_{kq}}{d\omega_t}$ is a generalized PDDCS. $C_{kq}(\theta_r, \phi_r)$ are modified

spherical harmonics. $\frac{1}{\sigma} \frac{d\sigma_{kq}}{d\omega_t}$ is a generalized PDDCS, and $\frac{1}{\sigma} \frac{d\sigma_{kq}}{d\omega_t}$ yields

$$\frac{1}{\sigma} \frac{d\sigma_{k0}}{d\omega_t} = 0 \text{ (k is odd),} \tag{17}$$

$$\frac{1}{\sigma} \frac{d\sigma_{kq+}}{d\omega_t} = \frac{1}{\sigma} \frac{d\sigma_{kq}}{d\omega_t} + \frac{1}{\sigma} \frac{d\sigma_{k-q}}{d\omega_t} = 0 \text{ (k even, q odd or k odd, q even),} \tag{18}$$

$$\frac{1}{\sigma} \frac{d\sigma_{kq-}}{d\omega_t} = \frac{1}{\sigma} \frac{d\sigma_{kq}}{d\omega_t} - \frac{1}{\sigma} \frac{d\sigma_{k-q}}{d\omega_t} = 0 \text{ (k even, q even or k odd, q odd).} \tag{19}$$

The PDDCS is written in the following form:

$$\frac{1}{\sigma} \frac{d\sigma_{kq\pm}}{d\omega_t} = \sum_{k_1} \frac{[k_1]}{4\pi} S_{kq\pm}^{k_1} C_{k_1-q}(\theta_t, 0), \tag{20}$$

where the $S_{kq\pm}^{k_1}$ is evaluated by using the expected value expression to be

$$S_{kq\pm}^{k_1} = \langle C_{k_1q}(\theta_t, 0) C_{kq}(\theta_r, 0) [(-1)^q e^{iq\phi_r} \pm e^{-iq\phi_r}] \rangle, \quad (21)$$

where the angular brackets represent an average over all angles. The differential cross-section is given by

$$\frac{1}{\sigma} \frac{d\sigma_{00}}{d\omega_t} = P(\omega_t) = \frac{1}{4\pi} \sum [k_1] h_0^{k_1}(k_1, 0) P_{k_1}(\cos\theta_t). \quad (22)$$

The bipolar moments $h_0^{k_1}(k_1, 0)$ are evaluated by using the expectation values of the Legendre moments of the differential cross-section and expressed as

$$h_0^{k_1}(k_1, 0) = \langle P_{k_1}(\cos\theta_t) \rangle. \quad (23)$$

The PDDCS with $q = 0$ is presented by

$$\frac{1}{\sigma} \frac{d\sigma_{k0}}{d\omega_t} = \frac{1}{4\pi} \sum [k_1] S_{k0}^{k_1} P_{k_1}(\cos\theta_t), \quad (24)$$

where $S_{k0}^{k_1}$ is evaluated by the expected value expression and given as

$$S_{k0}^{k_1} = \langle P_{k_1}(\cos\theta_t) P_k(\cos\theta_r) \rangle. \quad (25)$$

Many photon-initiated bimolecular reaction experiments are sensitive to only those polarization moments with $k = 0$ and $k = 2$. In order to compare calculations with experiments, PDDCS₀₀ ($\frac{2\pi}{\sigma} \frac{d\sigma_{00}}{d\omega_t}$), PDDCS₂₀ ($\frac{2\pi}{\sigma} \frac{d\sigma_{20}}{d\omega_t}$), PDDCS_{22+}} ($\frac{2\pi}{\sigma} \frac{d\sigma_{22+}}{d\omega_t}$), and PDDCS_{21-}} ($\frac{2\pi}{\sigma} \frac{d\sigma_{21-}}{d\omega_t}$) are calculated. In the above calculations, PDDCSs are expanded up to $k_1 = 7$, which is sufficient for good convergence.

3. Results and discussion

3.1 The k - j' vector correlation

The product $P(\theta_r)$ distribution describes the k - j' vector correlation with $k j' = \cos(\theta_r)$. Figure 2 displays the calculated $P(\theta_r)$ distributions of NH products from the $N(^2D) + H_2 \rightarrow NH + H$ reaction at collision energies $E_c = 2.0, 3.8, 5.1, 7.0, 9.0,$ and 11.0 kcal/mol. It is clear that the $P(\theta_r)$ distribution peaks at $\theta_r = 90^\circ$, and exhibits a very good symmetry with respect to 90° . This indicates that the product rotational angular momentum vector (j') is aligned along the direction at right angle to the relative velocity direction (k). With the collision energy increasing, the peak at $\theta_r = 90^\circ$ becomes small, which means that high

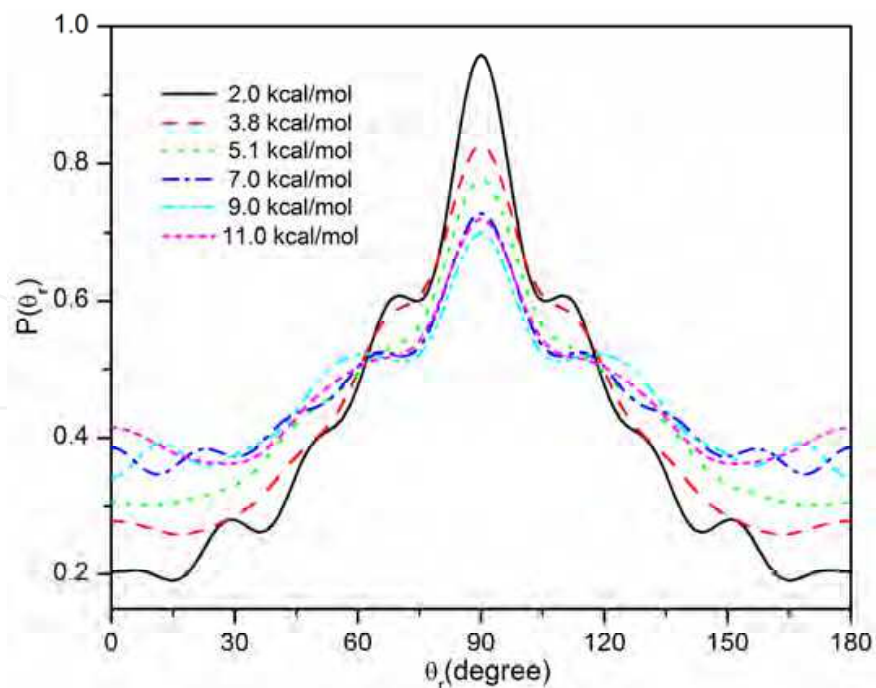


Fig. 2. $P(\theta_r)$ distributions for the NH products in the $N(^2D) + H_2(v=0, j=0) \rightarrow NH + H$ reaction at $E_c = 2.0, 3.8, 5.1, 7.0, 9.0,$ and 11.0 kcal/mol collision energies.

collision energy weakens the product rotational alignment. However, there is a very tiny exception that the $P(\theta_r)$ peak at $\theta_r = 90^\circ$ at 11.0 kcal/mol is a little bit smaller than that at 9.0 kcal/mol. The location and height of the barrier of the PES is related with the entrance and exit channels, which may be the reason of this tiny disagreement. Figure 3 shows the

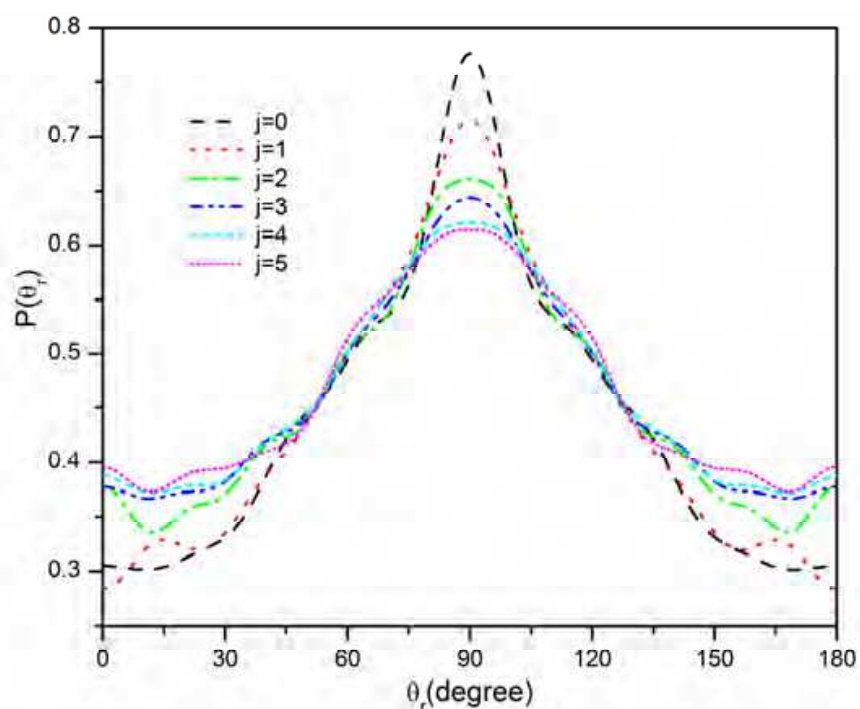


Fig. 3. $P(\theta_r)$ distributions for the NH products in the $N(^2D) + H_2(v=0, j=0, 1, 2, 3, 4, 5) \rightarrow NH + H$ reaction at $E_c = 5.1$ kcal/mol collision energy.

effect of the reagent rotational excitation on the product $P(\theta_r)$ distributions at collision energy of 5.1 kcal/mol. As clearly shown in Fig. 3, the higher the rotational excitation is, the smaller the $P(\theta_r)$ peak at $\theta_r = 90^\circ$. This indicates that the reagent rotational excitation depresses the product rotational alignment.

3.2 The $k-k'-j'$ vector correlation

Under the ϕ_r definition of the dihedral angle between the planes consisting of $k-k'$ and $k-j'$, the $P(\phi_r)$ distribution describes the $k-k'-j'$ vector correlation and can provide both product alignment and product orientation information. Figure 4 presents the product $P(\phi_r)$ distributions for the $\text{N}(^2\text{D}) + \text{H}_2(v=0, j=0) \rightarrow \text{NH} + \text{H}$ reaction at collision energies of 2.0, 3.8, 5.1, 7.0, 9.0, and 11.0 kcal/mol. As can be seen, in contrast to the symmetric feature of the $P(\theta_r)$ distribution with respect to $\theta_r = 90^\circ$, the $P(\phi_r)$ distribution is asymmetric with respect to the scattering plane where $\phi_r = 180^\circ$, but symmetric with respect to that where $\phi_r = 270^\circ$. The product $P(\phi_r)$ distribution behaves a large peak at $\phi_r = 270^\circ$ and a small peak at $\phi_r = 90^\circ$ for the $\text{N}(^2\text{D}) + \text{H}_2(v=0, j=0) \rightarrow \text{NH} + \text{H}$ reaction under each collision energy. Another two peaks emerge at about $\phi_r = 0^\circ$ and $\phi_r = 180^\circ$ when collision energy is 2.0 kcal/mol, which disappear in higher collision energies. The peaks at $\phi_r = 270^\circ$ for the higher collision energies are larger than that for the collision energy $E_c = 2.0$ kcal/mol, with the largest peak situated at the collision energy $E_c = 5.1$ kcal/mol. However, the peaks at $\phi_r = 90^\circ$ have no large change with the collision energy increasing. Therefore, we can conclude that the most NH product rotational angular momentum tend to align along the direction of y axis which is perpendicular to the scattering $k-k'$ plane, and orientate along the negative directions of y axis. That is to say, the product molecules prefer a counterclockwise rotation (see from the negative direction of y axis) in the plane parallel to the scattering plane.

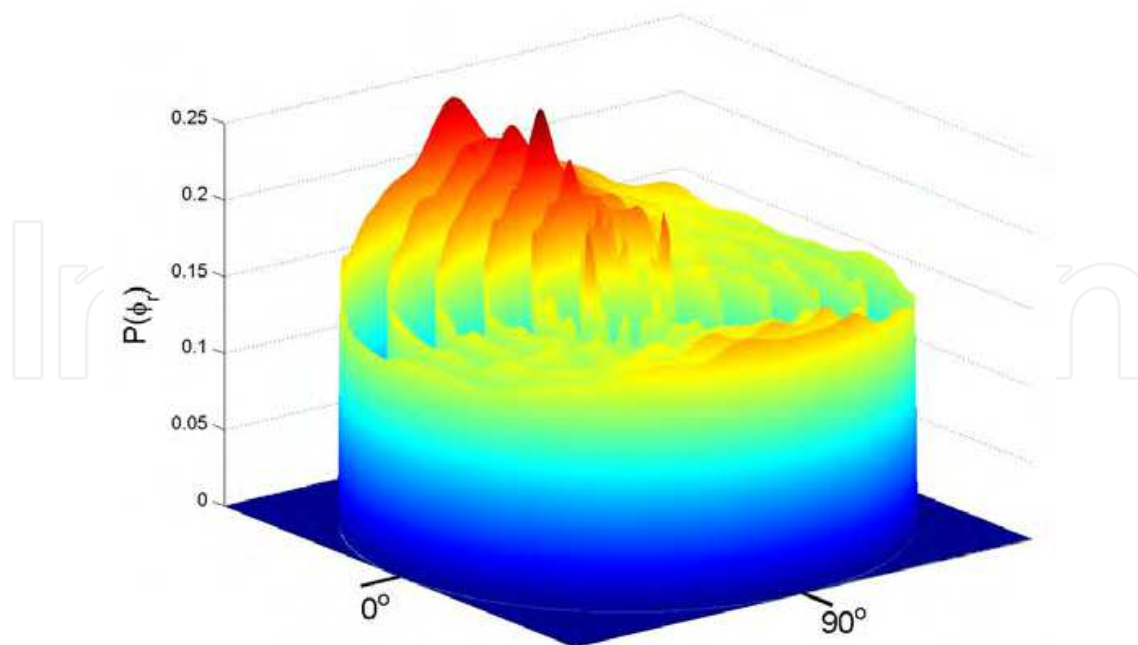


Fig. 4. $P(\phi_r)$ distributions as a function of the dihedral angle ϕ_r at collision energies of 2.0, 3.8, 5.1, 7.0, 9.0, and 11.0 kcal/mol (from inner to outer) for the $\text{N}(^2\text{D}) + \text{H}_2(v=0, j=0) \rightarrow \text{NH} + \text{H}$ reaction.

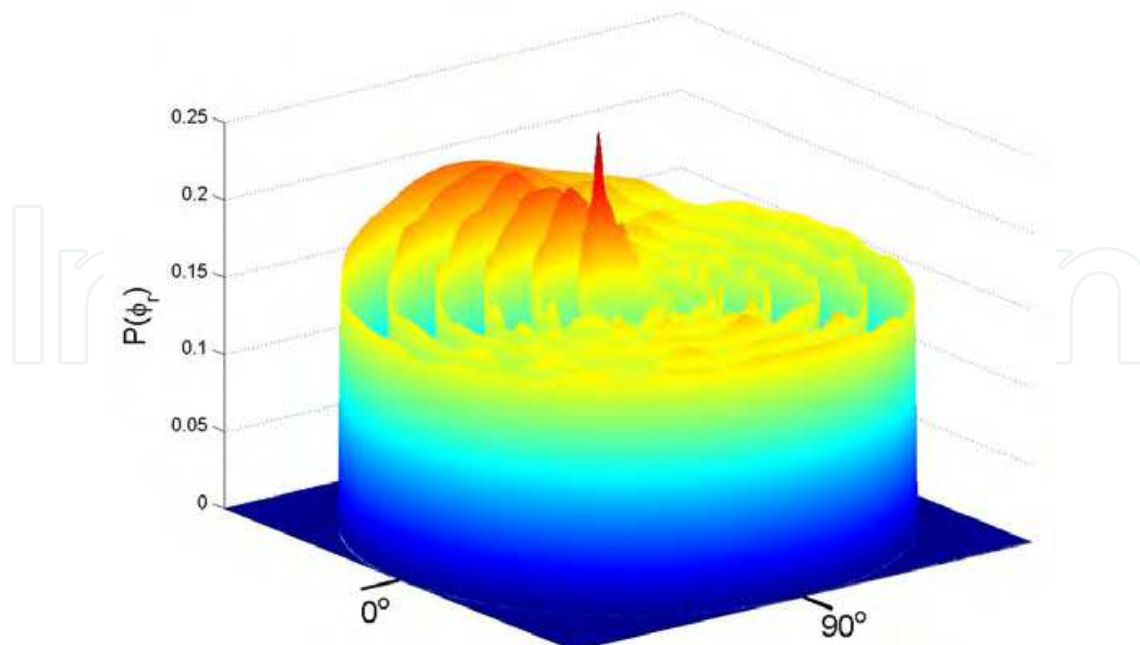
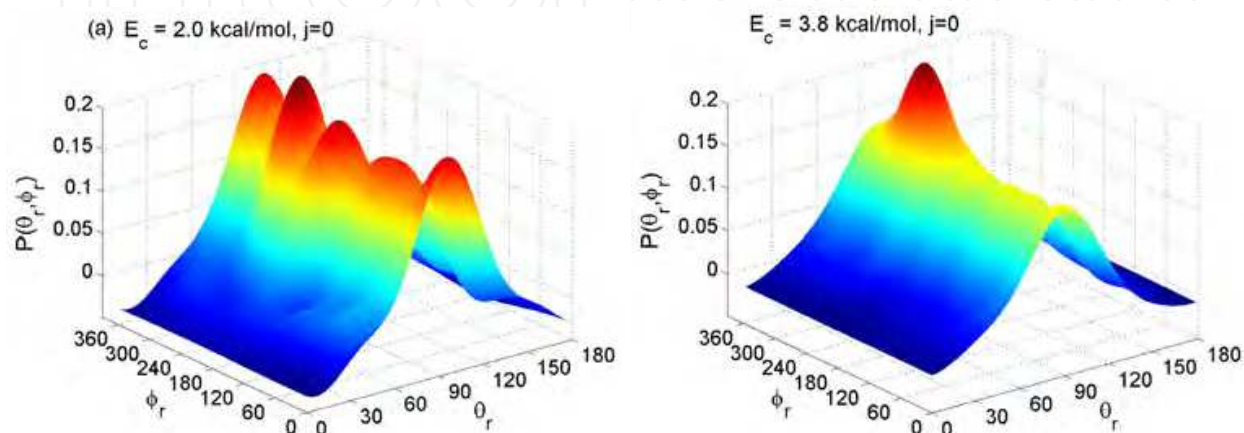
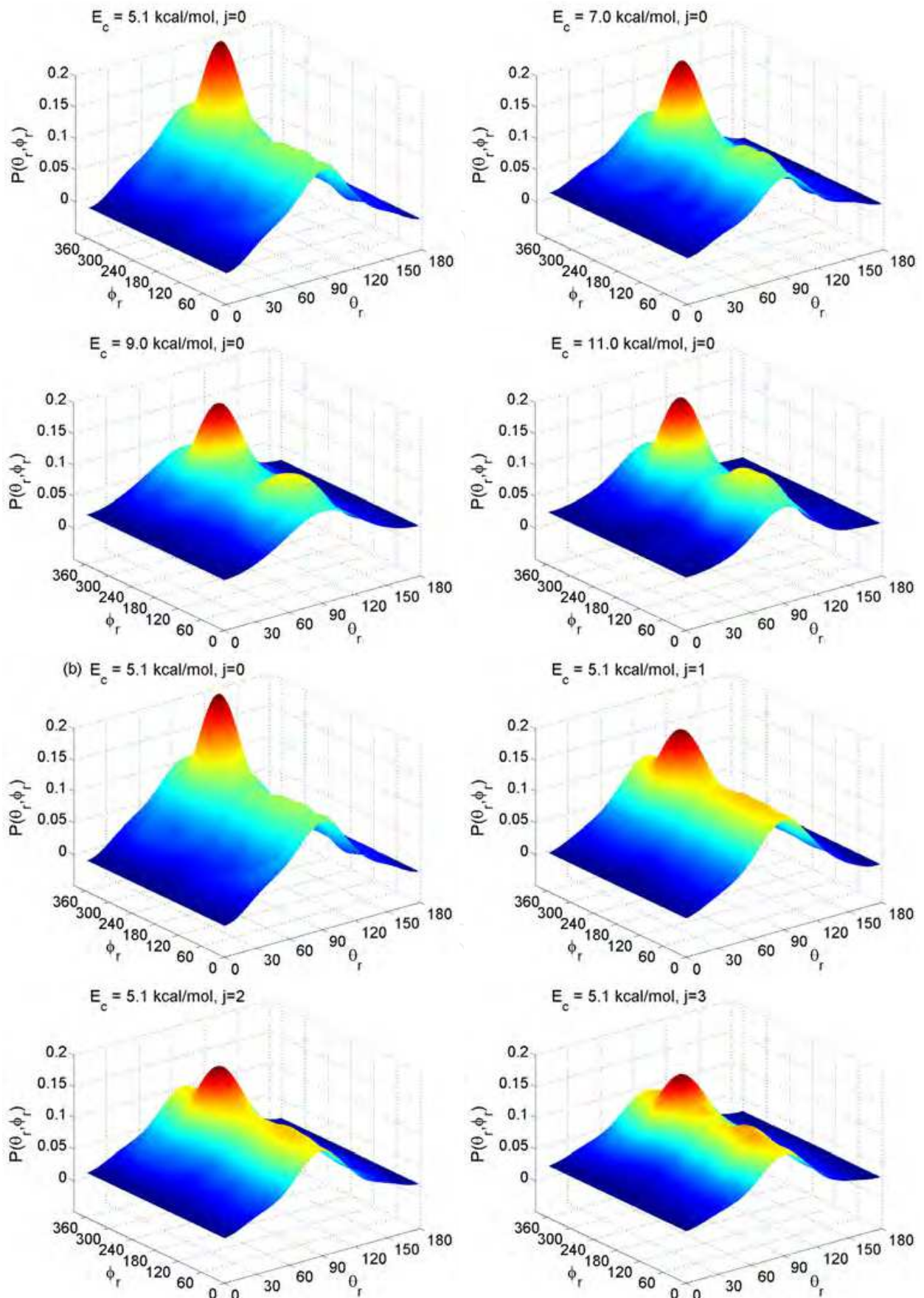


Fig. 5. $P(\phi_r)$ distributions as a function of the dihedral angle ϕ_r for the $\text{N}(^2\text{D}) + \text{H}_2(v=0, j=0, 1, 2, 3, 4, 5) \rightarrow \text{NH} + \text{H}$ reactions (from inner to outer) at the collision energy of 5.1 kcal/mol.

Figure 5 reveals the rotational excitation effect on the product $P(\phi_r)$ distributions for the $\text{N}(^2\text{D}) + \text{H}_2(v=0, j=0, 1, 2, 3, 4, 5) \rightarrow \text{NH} + \text{H}$ reactions at 5.1 kcal/mol collision energy. Obviously, all of the $P(\phi_r)$ distributions appear a large peak at about $\phi_r = 270^\circ$ and a small or no peak at about $\phi_r = 90^\circ$, which means that the orientation of the product rotational angular momentum tends to point to the negative direction of y axis. The peaks at about $\phi_r = 270^\circ$ for the $\text{N}(^2\text{D}) + \text{H}_2(v=0, j=1-5) \rightarrow \text{NH} + \text{H}$ reactions are smaller than that for the ground rotational state reaction, while there is very tiny change for the peaks at about $\phi_r = 90^\circ$. This indicates that the product rotational orientation becomes weaker when the reagent is excited to a higher rotational state.





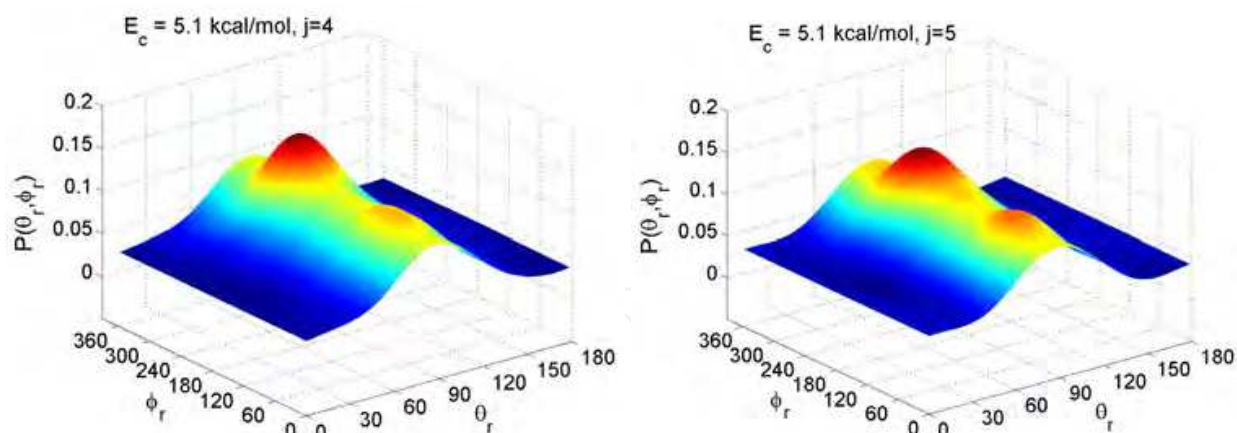


Fig. 6. $P(\theta_r, \phi_r)$ distributions as a function of both the polar θ_r and dihedral angle ϕ_r for the (a) $\text{N}(^2\text{D}) + \text{H}_2(v=0, j=0) \rightarrow \text{NH} + \text{H}$ reaction at collision energies of 2.0, 3.8, 5.1, 7.0, 9.0, and 11.0 kcal/mol, (b) $\text{N}(^2\text{D}) + \text{H}_2(v=0, j=0, 1, 2, 3, 4, 5) \rightarrow \text{NH} + \text{H}$ reactions at the 5.1 kcal/mol collision energy.

Further supporting information comes from the joint $P(\theta_r, \phi_r)$ distributions. Figure 6 presents the product $P(\theta_r, \phi_r)$ distributions for the $\text{N}(^2\text{D}) + \text{H}_2 \rightarrow \text{NH} + \text{H}$ reaction under different collision energies (Fig. 6a) and different reagent rotational excitations (Fig. 6b). The tomographical features are in good consistence with the separate $P(\theta_r)$ and $P(\phi_r)$ distributions. For example, the $P(\theta_r, \phi_r)$ distribution in the $\text{N}(^2\text{D}) + \text{H}_2(v=0, j=0) \rightarrow \text{NH} + \text{H}$ reaction at 2.0 kcal/mol collision energy has one largest peak at about $(\theta_r, \phi_r) = (90^\circ, 270^\circ)$, one small peak at about $(\theta_r, \phi_r) = (90^\circ, 90^\circ)$, and two medium peaks at about $(\theta_r, \phi_r) = (90^\circ, 0^\circ)$ and $(\theta_r, \phi_r) = (90^\circ, 180^\circ)$, respectively. These features reflect the characteristics of the $P(\theta_r)$ (Fig. 2) and $P(\phi_r)$ (Fig. 4) distributions for this concrete reaction. Similar things can be found for other specific reactions.

The atom (A) and diatomic molecule (BC) collision interaction can be described qualitatively by "Impulse model", [45] which applies the Newtonian mechanics and consider energy (e.g. endothermic translational, internal (rotational and vibrational), repulsive, and attractive energies) and momentum conservation. The QCT method simulates such interaction or reaction in the time domain step by step (time step, e.g. 0.1 fs) along each trajectory, where the energy and momentum conservations must be controlled from one step to the next step. Based on this impulsive model proposed for an $\text{A} + \text{BC} \rightarrow \text{AB} + \text{C}$ collision system in previous works, in the present system, the product angular momentum vector \mathbf{j}' can be written as $\mathbf{j}' = L \sin^2 \beta + j \cos^2 \beta + \mathbf{J}_1 m_B / m_{AB}$. Here L is the reagent orbital angular momentum and j is the reagent rotational angular momentum. $\mathbf{J}_1 = \sqrt{\mu_{BC} E_r} (\mathbf{r}_{AB} \times \mathbf{r}_{CB})$, with \mathbf{r}_{AB} and \mathbf{r}_{CB} being the unit vectors and B pointing to

A and C, respectively, μ_{BC} is the reduced mass of the BC molecule and E_r is the repulsive energy between B and C atoms. $\cos^2 \beta$ is the mass factor. With respect to the scattering plane, the first and second terms are symmetric terms, and thus the preferred direction of the product angular momentum is determined only by the third term of $\mathbf{J}_1 m_B / m_{AB}$, which is eventually traced back to the impulsive energy E_r of the collision system. As a consequence, we can say that the impulsive energy E_r leads to the preferred direction of the

product angular momentum vector. At a low collision energy of 2.0 kcal/mol, it seems that this effect of impulsive energy is not so evident, but it becomes more effective as collision energy increases, thus leading to the more preference for the counterclockwise rotation in the planes parallel to the scattering plane (Fig. 4). In the case of reactions for the reagent rotational excitation at collision energy of 5.1 kcal/mol, the alignment and orientation becomes weaker with the higher reagent rotational excitation. It is possibly because the rotational excitation weakens the impulsive energy E_r . However, the effect of collision energy and rotational excitation on the product rotational alignment and orientation is not always monotonic. As discussed in previous vector correlation studies, the product rotational alignment and orientation is also largely affected by the PES. [46-47] Therefore, the non-monotonic variety of the product alignment and orientation may be resulted by the PES.

3.3 The PDDCSs distributions

The generalized PDDCSs describe the k - k' - j' correlation and the scattering direction of the product molecule. Figure 7 shows the calculated results of the PDDCSs for the $N(^2D) + H_2(v=0, j=0) \rightarrow NH + H$ reaction under collision energies of 2.0, 3.8, 5.1, 7.0, 9.0, and 11.0 kcal/mol. The $PDDCS_{00}$ is simply proportional to the differential cross-section (DCS), and only describes the k - k' correlation or the product angular distributions. Figure 7a plots the $PDDCS_{00}$ as a function of scattering angle θ_t for the above reaction. Apparently, the $PDDCS_{00}$ shows a large peak at about $\theta_t = 180^\circ$ and a tiny peak at about $\theta_t = 0^\circ$ for the collision energy $E_c = 2.0$ kcal/mol, which means that the NH product angular distribution is almost the backward scattering. With the collision energy increasing, it shows a decreasing behavior for the peak at about $\theta_t = 180^\circ$, but a monotonously increasing behavior for the peak at $\theta_t = 0^\circ$. This indicates that the product angular distribution changes from the backward scattering to the both backward and forward scattering. Up to the collision energy $E_c = 11.0$ kcal/mol, both of the peaks at about $\theta_t = 180^\circ$ and 0° are nearly the same magnitude, which means that the NH product angular distribution is equally backward and forward scattering in the reaction. These results are in good agreement with recent exact QM results by Lin et al. [30]. The asymmetry in DCS was ascribed to the contributions of the fast insertion component of the reaction and the abstraction channel. The $PDDCS_{20}$ is the expectation value of the second Legendre moment $\langle P_2(\cos\theta_r) \rangle$ and contains the alignment information of j' with respect to k . As shown in Fig. 7b, the behaviour of the $PDDCS_{20}$ distribution demonstrates an opposite trend to that of $PDDCS_{00}$ and obviously depends on the scattering angle θ_t . It can be clearly seen from Fig. 7b that the $PDDCS_{20}$ values are negative for both backward and forward scatterings, but they are close to zero for sideways scattering. These results suggest that the j' polarizes preferentially along the direction perpendicular to k when the products are scattered forward and backward. This is consistent with the product alignment prediction from the $P(\theta_r)$ distribution shown in Fig. 2. Figure 7c and d illustrate the PDDCSs distributions with $q \neq 0$. All of the PDDCSs with $q \neq 0$ are equal to zero at the extremities of forward and backward scattering. The $PDDCS_{22+}$ value is positive or negative, depending on the preference of j' alignment along the x axis or y axis. It can be seen from Fig. 7c that the $PDDCS_{22+}$ values of the $N(^2D) + H_2(v=0, j=0) \rightarrow NH + H$ reaction at collision energies of larger than 2.0 kcal/mol are negative for all

scattering angles, which indicates that the alignments of the NH products prefer to be along the y axis. However, for the $N(^2D) + H_2(v=0, j=0) \rightarrow NH + H$ reaction at 2.0 kcal/mol, the $PDDCS_{22+}$ values are positive in the ranges of $\theta_t = 30^\circ \sim 73^\circ$, $83^\circ \sim 98^\circ$, and $140^\circ \sim 180^\circ$, with two largest positive peaks at $\theta_t = 55^\circ$ and 155° , respectively. These two positive peaks are corresponding with the $P(\phi_r)$ distributions (Fig. 4) in which there have two medium peaks at about $(\theta_r, \phi_r) = (90^\circ, 0^\circ)$ and $(\theta_r, \phi_r) = (90^\circ, 180^\circ)$ for the 2.0 kcal/mol collision energy. This demonstrates that the product j' alignment is not only along the y axis, but also along the x -axis. The $PDDCS_{21-}$ is related to $\langle -\sin 2\theta_r \cos \phi_r \rangle$, and its distribution is depicted in Fig. 7d. As shown in Fig. 7d, the $PDDCS_{21-}$ distribution shows a strongest polarization at about $\theta_t = 159^\circ$ for the $N(^2D) + H_2(v=0, j=0) \rightarrow NH + H$ reaction at 2.0 kcal/mol collision energy. Correspondingly, the $PDDCS_{21-}$ distributions show a medium polarization for collision energies of 3.8 and 5.1 kcal/mol at respect $\theta_t = 144^\circ$ and 140° , and a weak polarization for collision energies of 7.0, 9.0, and 11.0 kcal/mol corresponding with $\theta_t = 83^\circ$, 26° , and 18° . These results indicate that the product angular distributions are anisotropic for the $N(^2D) + H_2(v=0, j=0) \rightarrow NH + H$ reaction under each collision energy. The polarization degree becomes weaker with the increasing collision energy.

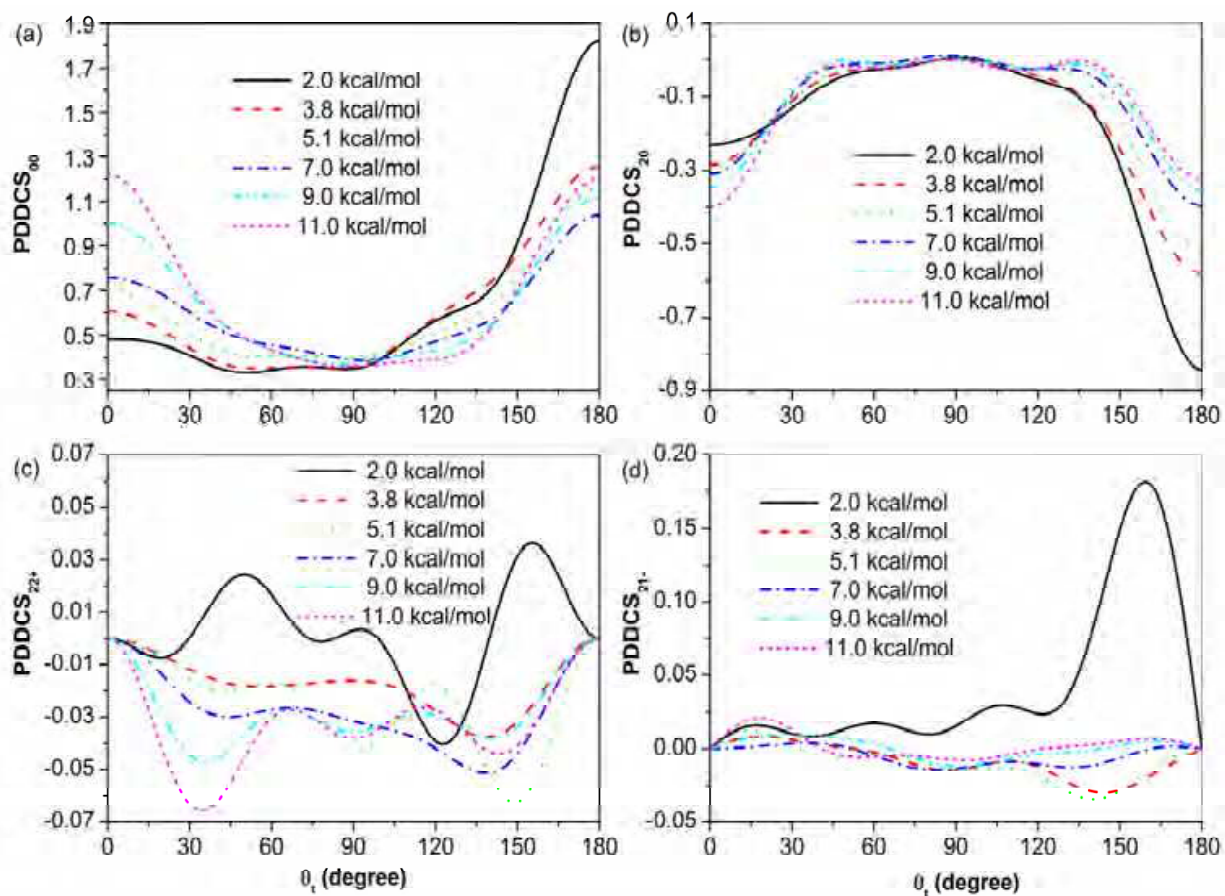


Fig. 7. (a) $PDDCS_{00}$, (b) $PDDCS_{20}$, (c) $PDDCS_{22+}$ and (d) $PDDCS_{21-}$ distributions as a function of scattering angle θ_t for the $N(^2D) + H_2(v=0, j=0) \rightarrow NH + H$ reaction at collision energies of 2.0, 3.8, 5.1, 7.0, 9.0, and 11.0 kcal/mol.

Figure 8 shows the rotational excitation effect on the PDDCSs distributions for the $N(^2D) + H_2(v=0, j=0-5) \rightarrow NH + H$ reactions at the 5.1 kcal/mol collision energy. As depicted in Fig. 8a, with the increasing rotational excitation, the peak at about $\theta_t = 180^\circ$ for the $PDDCS_{00}$ distribution becomes weaker, but stronger for the peak at about $\theta_t = 0^\circ$. These results mean that the rotational excitation leads to the product angular distribution changing from the backward scattering to the both backward and forward scattering. The $PDDCS_{20}$ distributions in Fig. 8b show negative values in both of the backward and forward scatterings, but they are close to zero for the sideways scatterings. These results suggest that the j' polarizes preferentially along the direction perpendicular to k , which is consistent with the product $P(\theta_\gamma)$ distributions in Fig. 3. The $PDDCS_{22+}$ values are negative for all scattering angles, meaning the alignments of the NH products prefer to be along the y axis. As can be seen from Fig. 8c, the rotational excitation diminishes the $PDDCS_{22+}$ peak, implying that the rotational excitation weakened the product alignment. The $PDDCS_{21-}$ distribution has two largest peaks for the $N(^2D) + H_2(v=0, j=0) \rightarrow NH + H$ reaction at $\theta_t = 15^\circ$ and 140° . However, no distinct large peaks were found in the $PDDCS_{21-}$ distribution for other rotational excited reactions. These characteristics illuminate that the rotational excitation reduce the anisotropy of the product angular distribution.

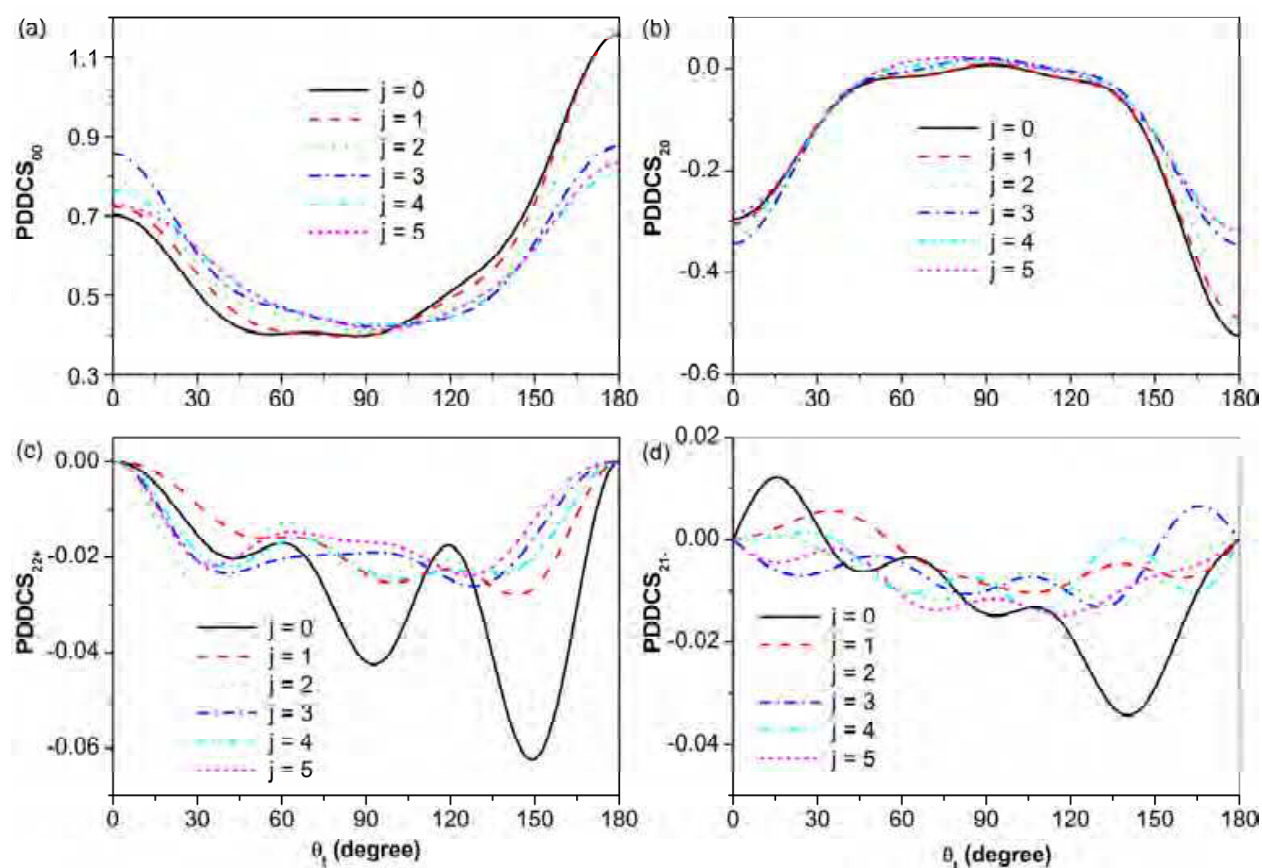


Fig. 8. (a) $PDDCS_{00}$, (b) $PDDCS_{20}$, (c) $PDDCS_{22+}$ and (d) $PDDCS_{21-}$ distributions as a function of scattering angle θ_t for the $N(^2D) + H_2(v=0, j=0, 1, 2, 3, 4, 5) \rightarrow NH + H$ reaction at the collision energy of 5.1 kcal/mol.

3.4 Rotational alignment parameter $A_0^{(2)}$

A simple way to express the degree of product rotational polarization of j' can be through the CM frame alignment parameter $A_0^{(2)} = 2\langle P_2(\mathbf{j}' \cdot \mathbf{K}) \rangle = \langle 3\cos^2\theta_r - 1 \rangle$, which is also a usual and common parameter measured in vector correlation experiments. [1] In this expression, the brackets denote an average over the distributions of j' with respect to \mathbf{K} . The product rotational alignment parameter $A_0^{(2)}$ has also been calculated at the present work, which is shown in Table 1. It can be seen from the $A_0^{(2)}$ expression that, for j' parallel or antiparallel to \mathbf{K} , $\langle P_2(\mathbf{j}' \cdot \mathbf{K}) \rangle = 1$ and then the alignment parameter takes the value $A_0^{(2)} = 2$, while for j' perpendicular to \mathbf{K} , $A_0^{(2)} = -1$. The values of the alignment parameter discussed above are limiting cases that represent the maximum possible alignment. In general, these parameters take values of small magnitude, which indicates a distribution that tends toward one of the above limits. If all alignment parameters are zero, the j' distribution is isotropic about \mathbf{K} . All of the $A_0^{(2)}$ values displayed in Table 1 are negative, which means that most of the product rotational angular momentum j' tend to be perpendicular to \mathbf{K} . For the $\text{N}(^2D) + \text{H}_2(v=0, j=0) \rightarrow \text{NH} + \text{H}$ reactions at collision energies of 2.0, 3.8, 5.1, 7.0, 9.0, and 11.0 kcal/mol, the $A_0^{(2)}$ value becomes larger with the collision energy increasing. For the $\text{N}(^2D) + \text{H}_2(v=0, j=0-5) \rightarrow \text{NH} + \text{H}$ reactions at the collision energy of 5.1 kcal/mol, the $A_0^{(2)}$ value also becomes larger with the rotational excitation increasing. These trends imply that both of the increasing collision energy and reagent rotational excitation depress the product rotational alignment. This is in good consistent with the the $P(\theta_r)$ distributions (Fig. 2 and 3).

E_c (kcal/mol)	J	b_{\max} (Å)	$A_0^{(2)}$
2.0	0	1.087	-0.39117
3.8		1.673	-0.22509
5.1		1.804	-0.21372
7.0		1.885	-0.21098
9.0		1.924	-0.21018
11.0		1.947	-0.21786
5.1	1	1.811	-0.22699
	2	1.811	-0.17626
	3	1.810	-0.14679
	4	1.817	-0.13044
	5	1.831	-0.13044

Table 1. Values of the impact parameters b_{\max} and product rotational alignment parameters $A_0^{(2)}$ calculated with 100, 000 trajectories for the $\text{N}(^2D) + \text{H}_2(v=0, j=0-5) \rightarrow \text{NH} + \text{H}$ reactions under collision energies of 2.0, 3.8, 5.1, 7.0, 9.0, and 11.0 kcal/mol.

4. Conclusion

In this chapter, we presented a detailed vector correlation study on the $N(^2D) + H_2(v=0, j=0-5) \rightarrow NH + H$ reaction at collision energies of 2.0, 3.8, 5.1, 7.0, 9.0, and 11.0 kcal/mol. Three angular distributions $P(\theta_r)$, $P(\phi_r)$, $P(\theta_r, \phi_r)$, and four PDDCSs were computed by the QCT method with a six-order symplectic integration. Under an accurate $1^2A''$ state PES, batches of 100,000 trajectories were running for the investigated reactions. It was found that the $P(\theta_r)$ distribution has a large peak at about $\theta_r = 90^\circ$, meaning that the product angular momentum j' is aligned perpendicular to k . With the collision energy increasing, for the $N(^2D) + H_2(v=0, j=0) \rightarrow NH + H$ reactions, the product rotational alignment becomes weaker due to the reduction of the $P(\theta_r)$ peak at about $\theta_r = 90^\circ$. Similarly, the rotational excitation also demonstrated a reducing behaviour for the product rotational alignment in the reactions of $N(^2D) + H_2(v=0, j=0-5) \rightarrow NH + H$ at 5.1 kcal/mol. However, the increasing collision energy enhanced the peak at about $\phi_r = 270^\circ$, demonstrating that the product rotational orientation was enhanced by the increasing collision energy. For the $N(^2D) + H_2(v=0, j=0-5) \rightarrow NH + H$ reactions at 5.1 kcal/mol, the rotational excitation reduced the $P(\phi_r)$ peak at about $\phi_r = 270^\circ$, and therefore depressed the product rotational orientation. The $P(\theta_r, \phi_r)$ distributions were consistent with the $P(\theta_r)$ and $P(\phi_r)$ distributions. These $P(\theta_r)$, $P(\phi_r)$ and $P(\theta_r, \phi_r)$ distributions had been interpreted by an "Impulsive model". At the low collision energy of 2.0 kcal/mol, the PDDCS₀₀ shows a large peak at about $\theta_t = 180^\circ$ and a very tiny peak at about $\theta_t = 0^\circ$ for the $N(^2D) + H_2(v=0, j=0) \rightarrow NH + H$ reaction, which indicates that the product angular distribution is the backward scattering. As the collision energy increasing, the product angular distribution changes from the backward scattering to the both backward and forward scatterings. Similar behavior was found for the rotational excitation which also leads to the product angular distribution changing from the backward scattering to the both backward and forward scatterings. The PDDCS₂₀ shows an opposite distribution to the PDDCS₀₀. The PDDCS₂₂₊ values in the investigated reactions are negative except for the $N(^2D) + H_2(v=0, j=0) \rightarrow NH + H$ reaction at 2.0 kcal/mol, meaning that most of the product angular momentum j' prefer to align along the y axis. This alignment was reduced by both of the increasing collision energy and rotational excitation. For the PDDCS₂₁ distribution, the collision energy increasing and reagent rotational excitation decreased the largest peaks, which indicate that the product rotational polarization is anisotropic. This anisotropic distribution was weakened by the rotational excitation and increasing collision energy. The calculated $A_0^{(2)}$ values reflect that the product rotational alignment is perpendicular to k , which is consistent with the aforementioned $P(\theta_r)$ distributions.

5. Acknowledgment

This work is supported by the National Natural Science Foundation of China (No. 21003062) and the Young Funding of Jining University (No. 2009QNKJ02).

6. References

- Alexander, A. J. et al. (2000). Product rotational angular momentum polarization in the reaction $O(^1D_2) + H_2 \rightarrow OH + H$. *Physical Chemistry Chemical Physics*, Vol.2, No.4, (February 2000), pp. 571-580, ISSN 1463-9076

- Aoiz, F. J. et al. (2004). Classical Stereodynamics in Ar + NO Inelastic Collisions. *Physical Chemistry Chemical Physics*, Vol.6, No.18, (September 2004), pp. 4407-4415, ISSN 1463-9076
- Aquilanti, V. et al. (2005). Orienting and Aligning Molecules for Stereochemistry and Photodynamics. *Physical Chemistry Chemical Physics*, Vol.7, No.2, (January 2005), pp. 291-300, ISSN 1463-9076
- Balucani, N. et al. (2001). Dynamics of the $N(^2D) + D_2$ Reaction from Crossed-Beam and Quasiclassical Trajectory Studies. *The Journal of Physical Chemistry A*, Vol.105, No.11, (February 2001), pp. 2414-2422, ISSN 1089-5639
- Balucani, N. et al. (2002). Quantum Effects in the Differential Cross Sections for the Insertion Reaction $N(^2D)+H_2$. *Physical Review Letters*, Vol.89, No.1, (July 2002), pp. 013201, ISSN 0031-9007
- Balucani, N. et al. (2006). Experimental and Theoretical Differential Cross Sections for the $N(^2D) + H_2$ Reaction. *The Journal of Physical Chemistry A*, Vol.110, No.2, (January 2006), pp. 817-829, ISSN 1089-5639
- Bañares L. et al. (2005). Influence of Rotation and Isotope Effects on the Dynamics of the $N(^2D)+H_2$ Reactive System and of Its Deuterated Variants. *The Journal of Chemical Physics*, Vol.123, No.22, (December 2005), pp. 224301, ISSN 3063-3070
- Barnwell, J. D. et al. (1983). Angular Correlations in Chemical Reactions. Statistical Theory for Four-vector Correlations. *The Journal of Physical Chemistry*, Vol.87, No.15, (July 1983), pp. 2781-2786, ISSN 1089-5639
- Brouard, M. et al. (2000). Product State Resolved Stereodynamics: Rotational Polarization of $OH(^2\Pi;v',N',\Omega,f)$ Scattered from the Reaction, $H+CO_2 \rightarrow OH+CO$. *The Journal of Chemical Physics*, Vol.113, No.8, (August 2000), pp. 3173-3180, ISSN 0021-9606
- Casavecchia, P. et al. (1999). Reactive Scattering of Oxygen and Nitrogen Atoms. *Accounts of Chemical Research*, Vol.32, No.6, (February 1999), pp. 503-511, ISSN 0001-4842.
- Castillo, J. F. (2007). Wave Packet and Quasiclassical Trajectory Calculations for the $N(^2D) + H_2$ Reaction and Its Isotopic Variants. *Chemical Physics*, Vol.332, No.1, (January 2007), pp. 119-131, ISSN 0301-0104
- Chen, M. D. et al. (2002). Theoretical studies of product polarization and state distributions of the $H + HCl$ reaction. *Chemical Physics*, Vol.283, No.3, (October 2002), pp. 463-472, ISSN 0301-0104
- Chen, M. D. et al. (2003). Theoretical Study of Stereodynamics for the Reactions $Cl+H_2/HD/D_2$. *The Journal of Chemical Physics*, Vol.118, No.10, (March 2003), pp. 4463-4470, ISSN 3063-3070
- Chu, T. S. (2009). Quantum Mechanics and Quasiclassical Study of the $H/D+FO \rightarrow OH/OD+F$, $HF/DF+O$ Reactions: Chemical Stereodynamics. *Journal of Computational Chemistry*, Vol.31, No.7, (October 2009), pp. 1385-1396, ISSN 0192-8651
- Chu, T. S. et al. (2006). A Quantum Wave Packet Dynamics Study of the $N(^2D) + H_2$ Reaction. *The Journal of Physical Chemistry A*, Vol.110, No.4, (February 2006), pp. 1666-1671, ISSN 1089-5639
- Fano, U. & Macek, J. H. (1973). Impact Excitation and Polarization of the Emitted Light. *Reviews of Modern Physics*, Vol.45, No.4, (October 1973), pp. 553-573, ISSN 0034-6861
- Han, K. L. et al. (1991). Chemical Reaction Dynamics of Barium Atom with Alkyl Bromides. *Chemical Physics Letters*, Vol.181, No.5, (July 1991), pp. 474-478, ISSN 0009-2614

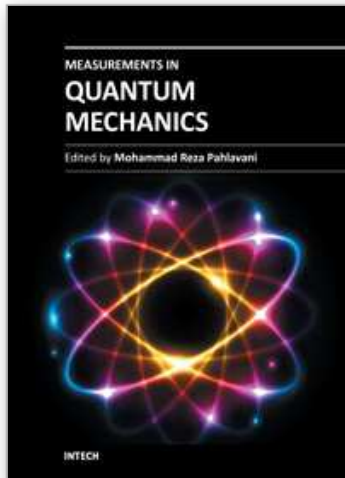
- Ho, T. S. et al. (2003). Implementation of a Fast Analytic Ground State Potential Energy Surface for the $N(^2D)+H_2$ Reaction. *The Journal of Chemical Physics*, Vol.119, No.6, (August 2003), pp. 9091-9100, ISSN 3063-3070
- Honvault, P. & Launay, J. M. (1999). A Quantum-mechanical Study of the Dynamics of the $N(^2D)+H_2 \rightarrow NH+H$ reaction. *The Journal of Chemical Physics*, Vol.111, No.15, (October 1999), pp. 6665-6667, ISSN 0021-9606
- Li, R. J. et al. (1994). Rotational Alignment of Product Molecules from the Reactions $Sr+CH_3Br$, C_2H_5Br , $n-C_3H_7Br$, $i-C_3H_7Br$ by Means of PLIF. *Chemical Physics Letters*, Vol.220, No.3-5, (April 1994), pp. 281-285, ISSN 0009-2614
- Lin, S. Y. & Guo, H. (2006). Exact Quantum Dynamics of $N(^2D)+H_2 \rightarrow NH+H$ Reaction: Cross-sections, Rate constants, and Dependence on Reactant Rotation. *The Journal of Chemical Physics*, Vol.124, No.3, (January 2006), pp. 031101, ISSN 3063-3070
- Lin, S. Y. et al. (2007). Differential and Integral Cross Sections of the $N(^2D) + H_2 \rightarrow NH + H$ Reaction from Exact Quantum and Quasi-Classical Trajectory Calculations. *The Journal of Physical Chemistry A*, Vol.111, No.12, (March 2007), pp. 2376-2384, ISSN 1089-5639
- M. Alagia, M. et al. (1999). Exploring the reaction dynamics of nitrogen atoms: A combined crossed beam and theoretical study of $N(^2D)+D_2 \rightarrow ND+D$. *The Journal of Chemical Physics*, Vol.110, No.18, (May 1999), pp. 8857-8860, ISSN 0021-9606
- Marinakos, S. et al. (2008). Rotational Angular Momentum Polarization: The Influence of Stray Magnetic Fields. *The Journal of Physical Chemistry*, Vol.128, No.2, (January 2008), pp. 021101, ISSN 1089-5639
- Mcclelland, G. M. & Herschbach, D. R. (1979). Symmetry Properties of Angular Correlations for Molecular Collision Complexes. *The Journal of Physical Chemistry*, Vol.83, No.11, (May 1979), pp. 1445-1454, ISSN 1089-5639
- Orr-Ewing, A. J. & Zare, R. N. (1994). Orientation and Alignment of Reaction Products. *Annual Review of Physical Chemistry*, Vol.45, (October 1994), pp. 315-366, ISSN 0066-426X
- Orr-Ewing, A. J. et al. (1997). Scattering-angle Resolved Product Rotational Alignment for the Reaction of Cl with Vibrationally Excited Methane. *The Journal of Chemical Physics*, Vol.106, No.14, (April 1997), pp. 5961-5971, ISSN 0021-9606
- Pederson, L. A. et al. (1999). Potential Energy Surface and Quasiclassical Trajectory Studies of the $N(^2D)+H_2$ Reaction. *The Journal of Chemical Physics*, Vol.110, No.18, (May 1999), pp. 9091-9100, ISSN 0021-9606
- Perkins, B. G. & Nesbitt, D. J. (2008). Stereodynamics in State-resolved Scattering at the Gas-Liquid Interface. *Proceedings of the National Academy of Sciences of the United States of America*, Vol.105, No.35, (September 2008), pp. 12684-12689, ISSN 0027-8424
- Rao, B. J. & Mahapatra, S. (2007). Quantum Wave Packet Dynamics of $N(^2D)+H_2$ Reaction. *The Journal of Chemical Physics*, Vol.127, No.24, (December 2007), pp. 244307, ISSN 3063-3070
- Schlier, C. & Seiter, A. (1998). Symplectic Integration of Classical Trajectories: A Case Study. *The Journal of Physical Chemistry A*, Vol.102, No.47, (July 1998), pp. 9399-9404, ISSN 1089-5639
- Schlier, C. & Seiter, A. (2000). High-order Symplectic Integration: An Assessment. *Computer Physics Communications*, Vol. 130, No.1-2, (July 2000), pp. 176-189. ISSN 0010-4655

- Shafer-Ray, N. E. et al. (1995). Beyond State-to-State Differential Cross Sections: Determination of Product Polarization in Photoinitiated Bimolecular Reactions. *The Journal of Physical Chemistry*, Vol.99, No.19, (May 1995), pp. 7591-7603, ISSN 1089-5639
- Stapelfeldt, H. & Seideman, T. (2003). Colloquium: Aligning Molecules with Strong Laser Pulses. *Reviews of Modern Physics*, Vol.75, No.2, (April 2003), pp. 543-557, ISSN 0034-6861
- Suzuki, T. et al. (1993). Reactions of N(2 ²D) and N(2 ²P) with H₂ and D₂. *Journal of the Chemical Society, Faraday Transactions*, Vol.89, No.7, pp. 995-999, ISSN 0956-5000
- Umemoto, H. & Matsumoto, K. (1996). Production of NH(ND) Radicals in the Reactions of N(2²D) with H₂(D₂): Nascent Vibrational Distributions of NH(X ³Σ⁻) and ND(X ³Σ⁻). *The Journal of Chemical Physics*, Vol.104, No.23, (June 1996), pp. 9640-9643, ISSN 0021-9606
- Umemoto, H. et al. (1997). Nascent Rotational and Vibrational State Distributions of NH(X ³Σ⁻) and ND(X ³Σ⁻) Produced in the Reactions of N(2 ²D) with H₂ and D₂. *The Journal of Chemical Physics*, Vol.106, No.12, (March 1997), pp. 4985-4991, ISSN 0021-9606
- Umemoto, H. et al. (2000). Verification of the Insertion Mechanism of N(2 ²D) into H-H Bonds by the Vibrational State Distribution Measurement of NH(X ³Σ⁻, 0 ≤ v'' ≤ 3). *The Journal of Chemical Physics*, Vol.112, No.13, (April 2000), pp. 5762-5766, ISSN 0021-9606
- Wang, M. L. et al. (1997). Reaction Dynamics of the Sr(3P_J) + RI → SrI* + R (R = CH₃, CH₃CH₂) Systems: Rotational Alignment, Electronic State Branching Ratio and Vibrational State Population of Products. *Chemical Physics Letters*, Vol.278, No.4-6, (October 1997), pp. 307-312, ISSN 0009-2614
- Wang, M. L. et al. (1998). Product Rotational Polarization in Photo-initiated Bimolecular Reactions A+BC: Dependence on the Character of the Potential Energy Surface for Different Mass Combinations. *The Journal of Physical Chemistry A*, Vol.102, No.50, (November 1998), pp. 10204-10210, ISSN 1089-5639
- Wang, M. L. et al. (1998). Product Rotational Polarization in the Photoinitiated Bimolecular Reaction A+BC→AB+C on Attractive, Mixed and Repulsive Surfaces. *The Journal of Chemical Physics*, Vol.109, No.13, (October 1998), pp. 5446-5454, ISSN 3063-3070
- Wright, A.N. & Winkler C.A. (1968). *Active Nitrogen*. Academic, ISBN 0127651500, New York
- Yue, X. F. et al. (2010). Quasi-Classical Trajectory Study of the Reactions N(2D) with H₂, D₂, and HD. *Journal of Theoretical and Computational Chemistry*, Vol.9, No.5, (October 2010), pp. 919-924, ISSN 0219-6336
- Yue, X. F. et al. (2010). Quasi-classical Trajectory Study of the N(2D) + H₂ → NH + H and N(2D) + D₂ → ND + D reactions: Vector Correlation. *Journal of Molecular Structure: THEOCHEM*, Vol.955, No.1-3, (September 2010), pp. 61-65, ISSN 2210-271X
- Yue, X. F. et al. (2010). Stereodynamics Study of the Reactions N(2D) + HD → NH + D and ND + H. *Chinese Physics B*, Vol.19, No.4, (April 2010), pp. 043401, ISSN 1674-1056
- Zhan, J. P. et al. (1997). Rotational Alignment of Products from the NOCl + Ca Chemiluminescent Reaction. *The Journal of Physical Chemistry A*, Vol.101, No.41, (October 1997), pp. 7486-7489, ISSN 1089-5639

Zhang, X. & Han, K. L. (2006). High-order Symplectic Integration in Quasi-classical Trajectory Simulation: Case Study for $O(^1D) + H_2$. *International Journal of Quantum Chemistry*, Vol.106, No.8, (July 2006), pp. 1815–1819, ISSN 0020-7608

IntechOpen

IntechOpen



Measurements in Quantum Mechanics

Edited by Prof. Mohammad Reza Pahlavani

ISBN 978-953-51-0058-4

Hard cover, 348 pages

Publisher InTech

Published online 22, February, 2012

Published in print edition February, 2012

Perhaps quantum mechanics is viewed as the most remarkable development in 20th century physics. Each successful theory is exclusively concerned about "results of measurement". Quantum mechanics point of view is completely different from classical physics in measurement, because in microscopic world of quantum mechanics, a direct measurement as classical form is impossible. Therefore, over the years of developments of quantum mechanics, always challenging part of quantum mechanics lies in measurements. This book has been written by an international invited group of authors and it is created to clarify different interpretation about measurement in quantum mechanics.

How to reference

In order to correctly reference this scholarly work, feel free to copy and paste the following:

Xian-Fang Yue (2012). Vector Correlations in Collision of Atom and Diatomic Molecule, Measurements in Quantum Mechanics, Prof. Mohammad Reza Pahlavani (Ed.), ISBN: 978-953-51-0058-4, InTech, Available from: <http://www.intechopen.com/books/measurements-in-quantum-mechanics/vector-correlations-in-collision-of-atom-and-diatomic-molecule>

INTECH
open science | open minds

InTech Europe

University Campus STeP Ri
Slavka Krautzeka 83/A
51000 Rijeka, Croatia
Phone: +385 (51) 770 447
Fax: +385 (51) 686 166
www.intechopen.com

InTech China

Unit 405, Office Block, Hotel Equatorial Shanghai
No.65, Yan An Road (West), Shanghai, 200040, China
中国上海市延安西路65号上海国际贵都大饭店办公楼405单元
Phone: +86-21-62489820
Fax: +86-21-62489821

© 2012 The Author(s). Licensee IntechOpen. This is an open access article distributed under the terms of the [Creative Commons Attribution 3.0 License](#), which permits unrestricted use, distribution, and reproduction in any medium, provided the original work is properly cited.

IntechOpen

IntechOpen